Collision effects in the nonlinear Raman response of liquid carbon disulfide

Thomas I. C. Jansen, Marcel Swart, Lasse Jensen, Piet Th. van Duijnen, and Jaap G. Snijders
Theoretical Chemistry, Materials Science Center, Rijksuniversiteit Groningen (RuG), Nijenborgh 4, 9747 AG Groningen, The Netherlands

Koos Duppen
Ultrafast Laser Laboratory, Materials Science Centre, Rijksuniversiteit Groningen (RuG), Nijenborgh 4, 9747 AG Groningen, The Netherlands

A model of the polarizability of carbon disulfide dimers was constructed, using polarizabilities from accurate time-dependent density functional theory calculations as reference. This direct reaction field model takes dipole-induced dipole effects, induced multipole effects and effects due to the overlap of the electronic clouds into account in an approximate way. The importance of the induced multipole and the overlap effects is investigated. This polarizability model is subsequently used to calculate the third-order time-domain Raman response of liquid carbon disulfide. These results are compared to experimental data and earlier calculated response in which only dipole-induced dipole effects on the polarizability were included. The multipole effects are found to give a significant contribution to the subpico second part of the third-order Raman response. © *2002 American Institute of Physics.* [DOI: 10.1063/1.1436463]

I. INTRODUCTION

Third-order time domain Raman experiments such as the (heterodyned) optical Kerr effect[1,2] and transient grating scattering[3,4] make it possible to observe the motion of atoms and molecules in liquids in real time. Since the response is determined by the time evolution of the first-order susceptibility, all motions that affect this susceptibility are observable. This includes intermolecular motions, and therefore Raman response techniques are very well suited to study the many-body aspects of motion in liquids, where intermolecular interactions play an important role.

The microscopic counterpart to the susceptibility is the polarizability, which can be calculated using quantum mechanical response methods such as time-dependent density functional theory (TDDFT). Unfortunately this method is far too time consuming to be used on large numbers of molecules as found in a molecular dynamics (MD) simulation. Alternatively polarizability models based on interacting molecular or atomic polarizabilities can be employed. In these models the physical interaction between the individual entities should be properly taken into account. The importance of different kinds of interactions can be studied by examining molecular dimers or small clusters of molecules.

Physical interactions between molecules, such as the dipole-induced dipole effect, induced multipole effects and electron cloud overlap effects, give rise to a polarizability deviating from the simple sum of the single molecule polarizabilities. The dipole-induced dipole effects arise from the fact that two molecules in a macroscopic electric field do not only feel the macroscopic field but also the field generated by the dipole induced on the other molecule. The induced-multipole effects arise because the molecules cannot be con-

sidered to have pointlike polarizabilities. Due to their extended atomic structure, the local field from induced dipoles on neighboring molecules does not need to be felt equally strong in both ends of a molecule. The electron cloud overlap effects arise from molecules so close to each other that their electron clouds overlap. The interaction between the overlapping electron clouds will also affect the polarizability.

In a number of previous studies[5–9] the dipole-induced dipole effects were included in the calculation of the nonlinear Raman response of liquid carbon disulfide. These effects were shown to be very important. They contribute with an intensity of similar magnitude as the signal arising from the independent single molecule polarizability. This indicates that the other intermolecular interactions could also be of importance to the observed optical response. On the other hand, the reasonably good agreement between the experimental results and the theoretical calculations, including only the dipole-induced dipole effects, seem to indicate that either the used polarizability model is sufficiently sophisticated or that the induced-multipole and electron overlap effects tend to cancel in the liquid. A few authors[7,10–12] have used atomic dipole-induced dipole polarizability models that include the induced-multipole effects in an approximative way. Reasonable agreement with experiment was found, but these models were not compared to quantum chemical calculations.

In this paper the contributions of induced-multipole and electron overlap effects to the third-order Raman response are investigated. For this purpose, a model was constructed that mimics these effects in dimers, where comparison between the model and accurate quantum calculations can be made. In Sec. II the calculation of the third-order Raman response from the first-order susceptibility, using molecular
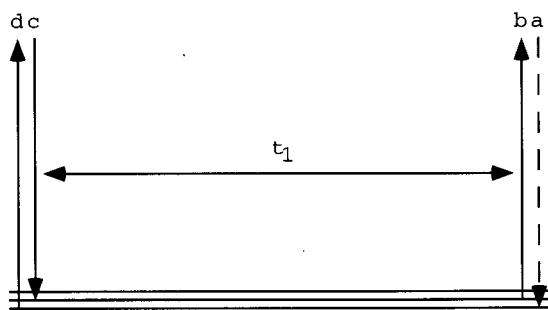
3277   © 2002 American Institute of Physics

FIG. 1. Third-order response energy level diagram. Here d, c, and b denote the polarization of the optical fields and a the polarization of the measured signal.

dynamics, will be briefly described. In Sec. III it will be shown how the first-order susceptibility can be found using the direct reaction field method. The results of the quantum and model calculations on dimers will be presented in Sec. IV. Then, in Sec. V the third-order Raman response functions of liquid carbon disulfide will be calculated with the different polarizability models. These theoretical results will be compared with experimental data. The conclusions are presented in Sec. VI.

II. NONLINEAR RAMAN RESPONSE

The third-order Raman experiment is governed by the third-order response function $\chi_{abcd}^{(3)}(t_1)$, where c and d denote the polarization directions of two initial laser fields perturbing the sample. After a delay t_1 the dynamics, following the impact of the initial interactions, is probed by a field with polarization direction b. This results in the emission of a signal field, which is detected with polarization direction a. In Fig. 1 an energy level diagram illustrating the third-order response is shown. It is important to realize that in a room temperature liquid a wide distribution of states is thermally occupied and that in the optical interactions dc and ba both upward and downward transitions occur.

The number of nonzero linear independent components of the third-order response is limited by symmetry. Since we investigate carbon disulfide, here the special case of linear molecules in an isotropic liquid will be considered. In that case only two nonzero linear independent components of the susceptibility exist.[13] These components can be chosen to be the polarized and depolarized components $\chi_{zzzz}^{(3)}$ and $\chi_{zxzx}^{(3)}$, respectively. Another choice is using the isotropic and anisotropic components, $\chi_{zzmm}^{(3)}$ and $\chi_{zxzx}^{(3)}$, respectively, where m denotes an axis forming an angle of 54.74° with the z-axis. This angle is often denoted the magic angle.

The isotropic component is related to the polarized and depolarized components through the relation:

$$\chi_{zzmm}^{(3)} = \chi_{zzzz}^{(3)} - \tfrac{4}{3}\chi_{zxzx}^{(3)}. \tag{1}$$

The anisotropic component is identical to the depolarized component. The isotropic and the anisotropic components contain information about fluctuations of the isotropic and anisotropic part of the susceptibility, respectively. Since the

polarized component is measured experimentally more often than the isotropic component, all three components $\chi_{zzzz}^{(3)}$, $\chi_{zxzx}^{(3)}$, and $\chi_{zzmm}^{(3)}$ will be treated here.

The third-order response functions can be expressed in terms of time correlation functions (TCFs). The third-order response function that governs the one-dimensional experiment depending on delay t_1, is given by the TCF of the first-order electronic susceptibility $\chi^{(1)}$, and its time derivative[5,8,9,14]

$$\chi_{abcd}^{(3)}(t) = -\frac{1}{2k_bT}\langle \dot{\chi}_{ab}^{(1)}(t)\chi_{cd}^{(1)}(0)\rangle. \tag{2}$$

This time correlation function can be calculated using Brownian oscillator models,[15,16] instantaneous normal mode data (INM) from snapshots in molecular dynamics simulations,[7,10,12,17] or full MD trajectories.[5,6,8,9,18–20]

The third-order response function can also be calculated using the finite field method (FF),[9,20] simulating the actual experiment. The forces, due to the optical fields E_c and E_d, at time zero, are applied to an equilibrated sample in the simulation and the response is measured by calculating the susceptibility $\chi_{ab;cd}^{(1)}(t)$ at later time steps. Numerous trajectories with different starting configurations are generated in order to produce sufficient statistical material. For each trajectory, the background noise $\chi_{ab;00}^{(1)}(t)$, from calculations without the applied forces, is subtracted to improve accuracy. To calculate the response, the duration of the applied laser pulses Δt and the number density N of the liquid has to be taken into account as well, which then gives the response:

$$\chi_{abcd}^{(3)}(t) = \frac{\chi_{ab;cd}^{(1)}(t) - \chi_{ab;00}^{(1)}(t)}{4\pi\epsilon_0 N E_c E_d \Delta t}. \tag{3}$$

One important reason for using the finite field method is that it is computationally cheaper to calculate the fifth-order response than the time correlation function methods.[9,20] The (two-dimensional) fifth-order response will not be treated in this paper.

The third-order response has often been fitted to different analytical models.[1,2,16,21–26] The following function describes the experimental results rather well,[21,22]

$$R(t) \propto (1 - \exp(-t/\tau_R) + A_R\sin(\Omega_R t)$$
$$\times \exp(-w_R t^2/2))\exp(-t/\tau_D). \tag{4}$$

Here, the constant τ_D is the diffusive relaxation time and the other constants are related to the initial subpicosecond part of the response. The Gaussian damped sine function is taken from the work by Kalpouzos *et al.*,[21,22] where it was related to the single-molecule librational motion.

The following expression, derived in frequency domain by Bucaro and Litovitz[23] for atomic collisions with zero impact parameter, describes the Raman response in terms of interaction induced effects,[23,24]

$$R(t) \propto \frac{\tau_C^n \sin(n\tan^{-1}(t/\tau_C))}{(t^2 + \tau_C^2)^{n/2}}. \tag{5}$$

The factor of τ_C^n was added here to eliminate the time unit dependence. The frequency domain response was originally given as

$$R(\omega) \propto \omega^{2[(m-7)/7]} \exp(-\omega/\omega_0), \qquad (6)$$

where ω_0 is the inverse of τ_C and $2[(m-7)/7]$ is equal to $n-1$ ($m=[7n+7]/2$). In the paper by Bucaro and Litovitz[23] the time constant τ_C was related to the molecular and thermodynamical properties in an approximate way,

$$\tau_C \approx \tfrac{1}{6}\pi r_0(\mu/kT)^{1/2}[1-(2/\pi)\tan^{-1}(2\epsilon/kT)^{1/2}]. \qquad (7)$$

Here ϵ and r_0 are the potential depth and the distance in a supposed Lennard–Jones potential and μ is the reduced mass. The constant m was related to the polarizability dependence on the interatomic distance r,

$$\alpha(r) - \alpha(\infty) \propto r^{-m}. \qquad (8)$$

It should be emphasized that one should be very careful using these functions for a microscopic interpretation of the liquid motion. The long time diffusive decay τ_D is the only constant that can be directly related to a dynamical property of the liquid. The description of the interaction induced effects, derived in an approximative way for atomic collisions, should be taken very cautiously or rather be avoided completely. The single molecule response is directly related to the time correlation function of the single molecule orientation tensor. This single molecule response is very difficult to isolate from experiments and fitting the results to a linear combination of Eqs. (4) and (5) will be likely to fail because of the similarity in shape between the Gaussian damped sine part of the single molecule response and the interaction induced response. In this way Kalpouzos et al.[21,22] succeeded in fitting the whole anisotropic response function to Eq. (4), while Hattori et al.[24] succeeded in fitting the anisotropic response function to the same equation, but leaving out the Gaussian damped sine part and including a contribution from Eq. (5) instead.

III. LOCAL-FIELD EFFECTS

In previous studies[5–9] local-field effects were taken into account in an approximate way, using molecular polarizabilities and including only the dipole-induced dipole interaction between the molecules. Thus, the molecules did not only feel the external electric field but also the electric fields generated by the induced dipoles in the surroundings. The surroundings were divided into two areas: the nearby environment with distinct local structure and the surroundings far away described by a continuous dielectric medium. The structured environment was limited to a spherical cavity around each individual molecule. To take the continuous dielectric medium into account, the macroscopic electric field was used instead of the external electric field. The contribution from the continuous dielectric medium inside the spherical cavity has to be eliminated in this scheme, by subtracting a term due to the polarization of a spherical dielectric medium.[9,14,27]

In the direct reaction field (DRF) method[28,29] the local field on an atom p is given by the macroscopic electric field E^{mac}, the electric fields generated by induced dipoles μ_q on atoms in a spherical cavity $\sum_{q\neq p}\mathcal{T}_{pq}\mu_q$ and a correction term subtracting the contribution from the same cavity filled with a continuum,[8,9,14,27]

$$E_p^{\mathrm{local}} = E^{\mathrm{mac}} + \sum_{p\neq q}\mathcal{T}_{pq}\mu_q + \frac{4\pi\chi^{(1)}}{3}E^{\mathrm{mac}}. \qquad (9)$$

For systems in vacuum the correction term proportional to the susceptibility of the surrounding medium vanishes.[28,29]

In order to treat the many-body interactions more properly than by the conventional dipole-induced dipole model, $\mathcal{T}_{pq}$ is a modified dipole field tensor defined as

$$\mathcal{T}_{pq} = \frac{3 f_{pq}^{T}(\hat{r}_{pq}:\hat{r}_{pq}) - f_{pq}^{E}}{r_{pq}^{3}}. \qquad (10)$$

The modification is present in the screening functions f_{pq}^{T} and f_{pq}^{E} which represent the damping due to overlapping charge densities. These screening functions are functions of the distance r_{pq} which approach one as r_{pq} goes to infinity, leaving the unmodified dipole tensor used to describe dipole-induced dipole effects. Various models for the screening functions have been suggested.[30] Assuming an exponentially decaying electron density around the atoms, one gets the following expressions for the screening functions:

$$\nu = \frac{\mathbf{a}r_{pq}}{(\alpha_p\alpha_q)^{1/6}}, \qquad (11)$$

$$f_{pq}^{E} = 1 - (\tfrac{1}{2}\nu^2 + \nu + 1)\exp(-\nu), \qquad (12)$$

$$f_{pq}^{T} = f_{pq}^{E} - \frac{\nu^3}{6}\exp(-\nu). \qquad (13)$$

The empirical screening factor $\mathbf{a}$, and the atomic polarizabilities are usually optimized to give as good a description of the molecular polarizability as possible for a wide variety of molecules.[29] This provides an empirical method that can be used to calculate the polarizability of other molecules.

Here, this approach will be employed to calculate the susceptibility of liquid CS$_2$. Three free parameters are present in the DRF model for CS$_2$. These are the isotropic polarizabilities on carbon and sulfur and the screening factor. For the first two, it will be required that the single molecule isotropic and anisotropic polarizabilities are exactly reproduced by the model. The screening factor was optimized by fitting to dimer calculations.

From the local-field expression a set of linear equations can be derived from which the polarizability of single molecules or dimers and the susceptibility of a liquid can be found.[5,6,9,29–31] This set of linear equations provides effective atomic polarizabilities Π_p that sum up to the total polarizability. This can be written as

$$\sum_p B_{qp}\Pi_p = L, \qquad (14)$$

where the B matrix is defined as

$$B_{qp} \equiv \alpha_q^{-1}\delta_{qp} - \mathcal{T}_{qp}(1-\delta_{qp}). \qquad (15)$$

L is the Lorentz factor, which without a surrounding liquid is one, while it is generally given by

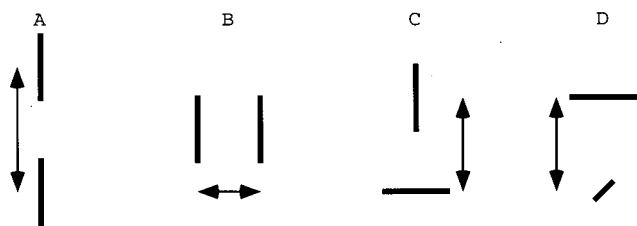$$L = 1 + \frac{4\pi\chi^{(1)}}{3}. \qquad (16)$$

FIG. 2. The four considered CS2 dimer configurations, A, B, C, and D. The intermolecular (center-of-mass) distances are marked with double arrows. The sloping line in configuration D indicates a molecule perpendicular to the paper plane.
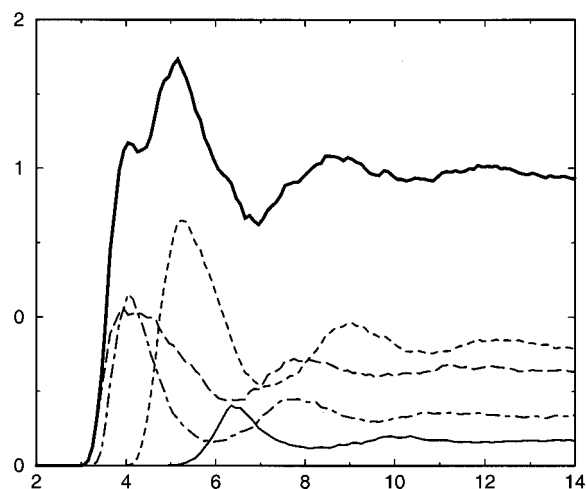

FIG. 3. The radial distribution functions for A (full), B (long dashed), C (dashed), and D (dashed-dotted) like dimer configurations (see FIG. 2) and the total radial distribution function (thick full).

The polarizability of a molecule or group of molecules in vacuum and the susceptibility of a liquid will then be given by the following summations

$$\Pi = \sum_p \Pi_p,$$
$$\chi^{(1)} = \frac{1}{V} \sum_p \Pi_p, \tag{17}$$

where V in the last case is the volume of the molecules in the model.

The interaction energy during the first Raman interaction is determined by the macroscopic optical fields E_a^{mac} and E_b^{mac} and the effective polarizabilities of the atoms[9,32]

$$H_{\mathrm{int}}^{ab} = -\frac{1}{2} \sum_p E_a^{\mathrm{mac}} \Pi_p E_b^{\mathrm{mac}}. \tag{18}$$

The force exerted in a given atomic coordinate x by the optical fields, is given by the derivative of the interaction energy with respect to that particular coordinate,

$$F_x^{ab} = -\frac{\partial H_{\mathrm{int}}^{ab}}{\partial x} \tag{19}$$

$$= \frac{1}{2} \sum_p E_a^{\mathrm{mac}} \frac{\partial \Pi_p}{\partial x} E_b^{\mathrm{mac}}. \tag{20}$$

So the force can be found if the derivatives of the effective atomic polarizabilities are known. These derivatives can be obtained by differentiating Eq. (14) which gives the set of linear equations

$$\sum_p B_{qp} \frac{\partial \Pi_p}{\partial x} = \sum_p \frac{\partial \mathcal{T}_{qp}}{\partial x} (1 - \delta_{qp}) \Pi_p. \tag{21}$$

The derivative of the modified dipole tensor is given in Appendix A.

In the calculations on liquid carbon disulfide, the sum over molecule pairs in the modified dipole interaction tensor has to be truncated so that only molecules within the cavity are taken into account. In the earlier calculations[9] this was a hard cutoff, where interaction at distances longer than the cut-off radius were set to zero and interactions at shorter distances were fully accounted for. In the calculations presented here a soft cutoff as described in Appendix B is introduced. The interaction is reduced continuously over a short distance around the cut-off radius, reducing artifacts that occur when molecules cross the boundary. The advantage of the soft cutoff is that the noise arising from molecules crossing the boundary is damped, allowing the use of shorter cut-off distances and faster calculations. In the limit where the cut-off radius goes towards infinity the two approaches are identical.

TABLE I. The DID and DRF models compared to the TDDFT results for dimers in the A configuration. The center-of-mass distances r_{CM}, are given in Å and the dimer polarizabilities in Å³.

A	1. axis (a)			2.+3. axes (b+c)			Abs. errors	
r_{CM}	DID	DRF	TDDFT	DID	DRF	TDDFT	DID	DRF
5	41.76	60.09	71.23	10.72	9.91	10.06	18.16%	6.21%
6	36.61	42.65	48.84	10.92	10.57	10.62	10.23%	4.54%
7	34.44	36.74	36.44	11.02	10.87	10.87	2.75%	0.27%
8	33.34	34.35	33.88	11.08	11.01	11.01	0.96%	0.46%
9	32.70	33.21	32.97	11.11	11.08	11.07	0.51%	0.30%
10	32.31	32.58	32.49	11.14	11.12	11.12	0.30%	0.09%
14	31.68	31.70	31.73	11.17	11.17	11.17	0.05%	0.03%
Av. Abs. error							4.7%	1.7%

J. Chem. Phys., Vol. 116, No. 8, 22 February 2002

Raman response of CS$_2$ 3281

TABLE II. The DID and DRF models compared to the TDDFT results for dimers in the B configuration. The center-of-mass distances r_{CM}, are given in Å and the dimer polarizabilities in Å^3.

B r_{CM}	1. axis (a)			2. axis (b)			3. axis (c)			Abs. errors	
	DID	DRF	TDDFT	DID	DRF	TDDFT	DID	DRF	TDDFT	DID	DRF
3	19.81	26.10	25.58	19.14	13.44	13.37	9.28	9.92	9.99	24.27%	1.09%
4	25.15	27.94	27.56	13.58	12.38	12.38	10.30	10.52	10.56	6.97%	0.75%
5	27.82	29.09	28.86	12.30	11.92	11.87	10.72	10.81	10.81	2.69%	0.41%
6	29.19	29.80	29.67	11.81	11.65	11.60	10.92	10.96	10.95	1.23%	0.32%
7	29.93	30.26	30.30	11.58	11.50	11.48	11.02	11.04	11.07	0.85%	0.19%
8	30.37	30.55	30.54	11.45	11.41	11.38	11.08	11.09	11.09	0.42%	0.10%
9	30.64	30.75	30.74	11.37	11.35	11.34	11.11	11.12	11.12	0.23%	0.04%
Av. Abs. error										5.2%	0.4%

IV. INTERMOLECULAR INTERACTIONS

Time dependent density functional theory (TDDFT) calculations have been performed on the carbon disulfide monomer as well as on dimers using the Amsterdam Density Functional Program Package (ADF).[33–38] The LB94 potential[39] has been used for the response calculations to ensure correct asymptotic behavior in the diffuse region. A Slater-type orbital function basis set of triple zeta quality with polarization and diffuse functions was employed (ADF basis set VIII constructed for polarization calculations). All calculations were done using an electric field frequency corresponding to a wavelength of 514.5 nm. For the calculations a C–S bondlength of 1.5704 Å was used.

The monomer polarizability was found to be 8.95 Å^3 while the anisotropy was found to be 10.05 Å^3. These values coincide with the experimental numbers reported by Bogaard et al.[40] This exact agreement is a matter of coincidence rather than evidence of the general accuracy of the method. In calculated polarizabilities using the TDDFT method absolute average deviations of 3.6% compared with experiment have been reported for a series of molecules.[41]

Four representative dimer configurations have been selected for investigation. These are shown in Fig. 2. The polarizabilities were calculated with TDDFT for these configurations at various intermolecular separations. Both the dipole-induced dipole approach and the DRF model, described in Sec. III, were used. In the DID model the molecular isotropic polarizability was 8.95 Å^3 and the molecular anisotropic polarizability was 10.05 Å^3. For the DRF model

the screening factor is set to 2.5568 and the atomic polarizabilities were set to 1.197024 and 3.00098 Å^3 for carbon and sulfur, respectively. This choice gives the correct polarizability for the monomer and the chosen screening factor gives an optimal description of the polarizability in the B and D configurations in the second solvation shell as will be described later.

The relative importance of the different configurations in the simulated liquid has been estimated by calculating the radial distribution function (RDF) using molecular dynamics. All dimer configurations in the liquid have been attributed to the configuration that they closest resemble. The RDFs for the dimer configurations and the total RDF are shown in Fig. 3.

The dimer polarizabilities are calculated at distances found realistic by examining the RDFs. For each dimer configuration the distances covering the two first peaks (solvation shells) in the RDF are included. Furthermore, in all configurations the polarizability is calculated in a point with shorter distance between the molecules than found in the RDF for that configuration. In Tables I–IV the polarizabilities obtained using the DID model and the DRF model are compared with the dimer polarizabilities calculated with TDDFT. The dimer polarizability is listed for the principal axes a, b, and c of the polarizability tensor. For configuration A, B, and D the DRF model is clearly better than the DID approach. For configuration C no improvement is found in the dimer polarizability using the DRF model. For this configuration the results even seem a bit worse than the DID

TABLE III. The DID and DRF models compared to the TDDFT results for dimers in the C configuration. The center-of-mass distances r_{CM}, are given in Å and the dimer polarizabilities in Å^3.

C r_{CM}	1. axis (a)			2. axis (b)			3. axis (c)			Abs. errors	
	DID	DRF	TDDFT	DID	DRF	TDDFT	DID	DRF	TDDFT	DID	DRF
4	29.23	27.31	31.44	18.92	19.35	21.69	10.30	10.08	10.24	6.80%	8.50%
5	24.61	24.48	25.58	19.96	2.01	19.90	10.72	10.59	10.62	1.68%	1.71%
6	23.05	23.10	23.07	20.48	20.46	20.40	10.92	10.85	10.85	0.37%	0.14%
7	22.34	22.38	22.28	20.75	20.73	20.75	11.02	10.99	11.00	0.15%	0.21%
8	21.96	22.99	21.95	20.91	20.90	20.90	11.08	11.07	11.07	0.06%	0.06%
9	21.75	21.76	21.74	21.01	21.00	21.00	11.11	11.10	11.10	0.06%	0.03%
10	21.61	21.62	21.61	21.08	21.07	21.07	11.14	11.13	11.12	0.08%	0.05%
Av. Abs. error										1.3%	1.5%

TABLE IV. The DID and DRF models compared to the TDDFT results for dimers in the D configuration. The center-of-mass distances r_{CM}, are given in Å and the dimer polarizabilities in $Å^3$.

D	1. axis (a)			2.+3. axes (b+c)			Abs. errors	
r_{CM}	DID	DRF	TDDFT	DID	DRF	TDDFT	DID	DRF
3	16.77	19.16	19.02	19.14	12.61	12.50	25.59%	0.78%
4	18.92	19.89	19.79	13.58	12.18	12.14	6.88%	0.45%
5	19.96	20.37	20.31	12.30	11.84	11.80	2.56%	0.31%
6	20.48	20.67	20.65	11.81	11.62	11.66	0.98%	0.18%
7	20.75	20.85	20.86	11.58	11.49	11.50	0.58%	0.06%
8	20.91	20.97	20.96	11.45	11.40	11.40	0.31%	0.03%
9	21.01	21.04	21.04	11.37	11.35	11.34	0.18%	0.03%
Av. Abs. error							5.3%	0.3%

result. In general the errors in both the DID and the DRF are less than 1% for distances in the order of the second solvation shell. In the first solvation shell the errors for the DID model are larger: up to 10% is found. In contrast, for the DRF model the results are still good, with errors in the B and D configurations of less than 1%. In the A and C configurations the errors are slightly larger.

The DRF model includes both the multipole and electron overlap contributions in an approximative way. From the results it is not immediately clear what the relative importance of these two contributions is. To get an idea about that, one can set the screening factors to one for interactions between atoms in different molecules, leaving only the effect of the multipole contribution between the dimers. In Table V this multipole model is compared with the DRF model for the A configuration as a representative example. The lack of intermolecular screening factors has a vanishing effect at separations larger than those found in the first solvation shell. Inside the first solvation shell of the A configuration the effect of the electron overlap is still rather small compared to the multipole effect. At very short distances, where the distance between the sulfur atoms is much smaller than twice the van der Waals radius, this multipole model breaks down and even gives unphysical negative polarizabilities. However, this only happens at distances shorter than those found in the MD simulations, which indicates that the major part of the correction is due to the multipole effects and not to the electron overlap effect.

The dipole–octupole polarizability of carbon disulfide monomers can be calculated using TDDFT.[42] Two independent components α_z^{30} and α_x^{31c} exist.[43] These were calculated

to be 53.03 and 29.29 $Å^5$, respectively, using TDDFT. From an expansion of the DRF expression for a single CS_2 molecule the dipole–octupole polarizability can also be estimated and values of 81.53 and 30.93 $Å^5$ are found. The discrepancy between the calculated and modeled α_z^{30} components explains some of the deviation between the DRF model and the TDDFT calculations.

The screening factor used was chosen by optimizing to the B and D dimer configurations in the second solvation shell that is dependent on the α_x^{31c} component. For this purpose the POLAR program by Swart and van Duijnen[28] was used. The DRF model employed here does not allow optimization to both the α_z^{30} and the α_x^{31c} component since it only contains three free variables in the case of CS_2, and two of these are used to give the correct single molecule polarizability components.

In principle, the static electric fields can also influence the polarizability through the hyperpolarizabilities. In the case of CS_2 the most relevant contribution is a combination of the electric field generated by the permanent quadrupole on CS_2 and the second hyperpolarizability γ. Such effects are neglected here but the good agreement between the TDDFT calculations and the DRF model indicates that this is a safe approximation.

V. MOLECULAR DYNAMICS

The MD simulations have been performed in the same way as described in earlier papers,[9,20] but with a simulation box that includes only 64 CS_2 molecules (192 atoms). The lower number of molecules is used to make the calculations

TABLE V. The importance of the multipole effects (M.Pol) and the electron overlap effects (E.O.) in the A configuration estimated from the DID, POL, and DRF models discussed in the text. At center-of-mass distances r_{CM} around 6.5 Å the sulfur atoms start touching each other.

A	1. axis (a)						2.+3. axes (b+c)					
r_{CM}	DID	POL	DRF	TDDFT	M.Pol	E.O.	DID	POL	DRF	TDDFT	M.Pol	E.O.
5	41.76	−68.75	60.09	71.23	−110.51	128.84	10.72	9.57	9.91	10.06	−1.15	0.34
6	36.61	47.36	42.65	48.84	10.75	−4.71	10.92	10.52	10.57	10.62	−0.40	0.05
7	34.44	37.15	36.74	36.44	2.71	−0.41	11.02	10.86	10.87	10.87	−0.16	0.01
8	33.34	34.40	34.35	33.88	1.06	−0.05	11.08	11.01	11.01	11.01	−0.07	0.00
9	32.70	33.21	33.21	32.97	0.51	0.00	11.11	11.08	11.08	11.07	−0.03	0.00
10	32.31	32.59	32.58	32.49	0.28	−0.01	11.14	11.12	11.12	11.12	−0.02	0.00
14	31.68	31.70	31.70	31.73	0.02	0.00	11.17	11.17	11.17	11.17	0.00	0.00

FIG. 4. The anisotropic response in units of 10^{-20} C^4 m/J^3 s.
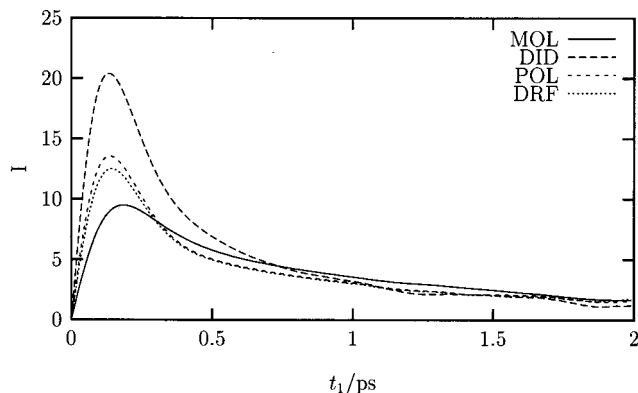
FIG. 6. The isotropic response in units of 10^{-20} C^4 m/J^3 s.

faster. Calculations with the DID model have been performed with both 64 and 256 molecule simulation boxes to verify that using a smaller box does not affect the results. The RDF referred to in the last section is taken from the calculations with 256 molecules. The cut-off distance is set to 20 Å and the interaction is softly reduced over a 0.2 Å thick region, using the method described in Appendix B.

Calculations containing only the single molecule reorientational response (MOL) have been done as well as calculations with the DID, the pure multipole model (POL) and DRF model including multipole and electron overlap effects. The anisotropic responses are shown in Fig. 4. Comparing the single molecule result (MOL) with the other responses makes it evident that the subpicosecond peak is dominated by interaction induced response and that these effects cannot be neglected. The difference between the response calculated using the DID model with the POL response shows that the multipole effects are also quite important. The difference between the POL and DRF model responses is limited, showing the smaller effect of the close collision electron overlap effects.

In Fig. 5 the same responses are shown but now normalized to peak height and together with the experimental response obtained by Steffen et al.[16] In the subpicosecond peak area the DID, POL, and DRF models all look very similar to the experimental response. In the long tail the DID
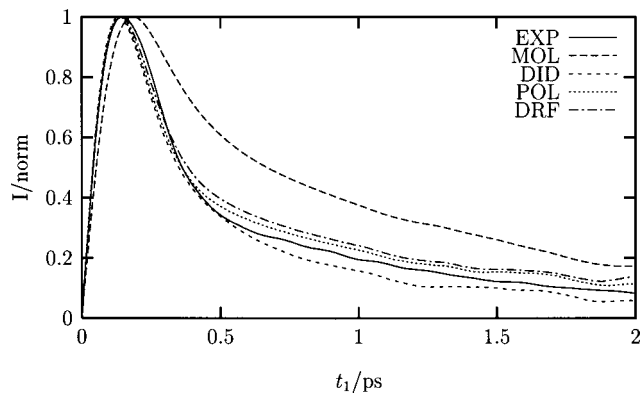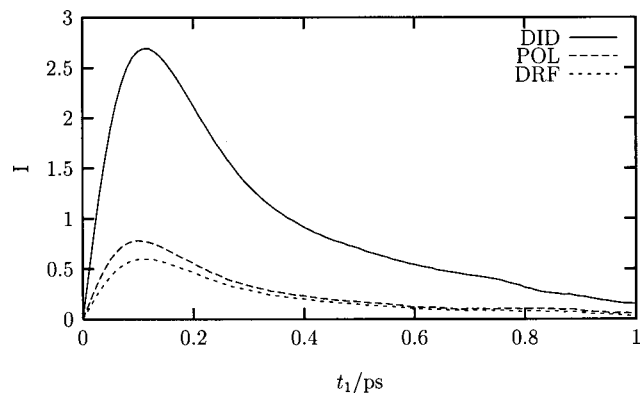
response is somewhat lower than the experimental response whereas the POL and DRF are higher. This means that the DID model overestimates the ratio between the interaction induced effects and the single molecule response, and the POL and DRF models to a lesser extent underestimate this ratio.

In Fig. 6 the isotropic responses are shown. The single molecule contribution to this component is zero, so all response is originating from the interaction induced many-body effects. A huge difference is observed between the DID model and the models including multipole effects. Again the DID model is overestimating the interaction induced response. Unfortunately, there are no reliable experimental results to compare with since the intensity is much smaller than the anisotropic response. Measurements by Blank et al.[44] just showed a very weak shoulder on the electronic response. Recent measurements[45–48] show promise for a more accurate measurement of the isotropic response.

To give a quantitative comparison between the different calculations, the responses have been fitted to the functions given in Eqs. (4) and (5). In these fits it is assumed that the shape of the single molecule response is not dependent on the model used to describe the interaction induced effects. The magnitude of the single molecule response is allowed to vary slightly. The results are shown in Table VI. The single molecule (MOL) response has been fitted to Eq. (4) and the fit constants τ_D, τ_R, A_R, Ω_R and w_R determining the shape of the single molecule response are kept fixed for the fits to the DID, POL, and DRF results, while the constant I_D determining the intensity is allowed to vary. No single molecule response is present in the isotropic response. From these fits it is seen that for the anisotropic response there is a big difference between the DID model and the models including the multipole effect. This is seen both in the I_C parameter characterizing the intensity and the τ_C and n parameters characterizing the shape of the interaction induced response. For the isotropic response the main difference is in the parameter characterizing the intensity. The ratio between the peak intensity of the anisotropic and the isotropic response changes dramatically from 7.57 in the DID model to 21.0 in the DRF model. These ratios provide a sensitive test that can be determined experimentally.

For the single molecule response the librational part is

FIG. 5. The anisotropic response normalized to one at the peak position.

TABLE VI. The fit constants for the calculated single molecule [Eq. (4)] and interaction induced [Eq. (5)] response, with I_D and I_C giving the intensities. No single molecule response is present in the isotropic response which is therefore fitted to the interaction induced expression [Eq. (5)] with I_C as intensity.

| | Anisotropic | | | | | | | | | Isotropic | | |
| | Single Molecule | | | | | | Inter. Ind. | | | Inter. Ind. | | |
	I_D	τ_D	τ_R	A_R	Ω_R	w_R	I_C	τ_C	n	I_C	τ_C	n
MOL	8.32	1.20	0.117	6.19	0.803	31.7	$\cdots$	$\cdots$	$\cdots$	$\cdots$	$\cdots$	$\cdots$
DID	5.88	–‖–	–‖–	–‖–	–‖–	–‖–	22.26	0.183	1.83	4.506	0.156	1.53
POL	7.39	–‖–	–‖–	–‖–	–‖–	–‖–	8.09	0.306	3.06	1.312	0.137	1.50
DRF	7.26	–‖–	–‖–	–‖–	–‖–	–‖–	6.66	0.309	3.09	0.985	0.165	1.63

found to be close to critically damped, while the A_R and Ω_R parameters can be varied quite a bit without changing the function too much, as long as the product of these two constants is kept fixed. The diffusional constant τ_D is found to be 1.20 ps, which is somewhat lower than the value 1.6 ps typically reported.[1,21,24,25,49] This is probably because the calculated response is truncated at 2 ps and the long tail domain is not really included. This gives an uncertainty in the diffusional constant τ_D that may be partly due to compensation of the errors in the librational part of the response.

VI. CONCLUSIONS

The DRF model was used to improve the dipole-induced dipole description of the dimer polarizabilities of carbon disulfide by including induced-multipole and electron overlap effects. This improved the quality of the theoretical description considerably. The fact that the DRF model did not model the dipole–octupole interactions correctly leaves some room for improvement. It was shown that both the induced-multipole and electron overlap effects are important for the third-order Raman response. The induced-multipole effects turned out to be the most important of the two.

The calculated third-order response was found to resemble the experimental response very well. The intensity of the initial response is overestimated somewhat in the DID model, while it is underestimated in the DRF model. In the isotropic response the inclusion of the induced-multipole effects were seen to reduce the intensity considerably with a factor of about four. From this substantial difference it must be concluded that the induced-multipole effects should be included when one calculates the isotropic third-order response, especially.

The observed rather small deviation between the response calculated using the DRF method and the experimental response does not need to originate only from the small remaining differences between the modeled and calculated polarizabilities. The fact that the force field used in the MD simulations is rather simple can also give rise to deviations. A molecular force field consisting of isotropic atomic Lennard–Jones potentials cannot give rise to the anisotropic asymptotical behavior that is present in anisotropic molecules as CS_2, but only mimic the anisotropy in the force field at short distances.[50] Furthermore in the force field used the relatively large quadrupole moment in CS_2 is ignored.

The effects observed in this study surely will also have implications on the calculated higher-(fifth)-order Raman re-

sponse that is known to be even more sensitive to the interaction induced effects than the third-order response.[7,9,51] This will be a subject of further study.

APPENDIX A: DERIVATIVES

To find the derivatives of the effective polarizabilities as given in Eq. (21) the derivatives of the modified dipole tensor must be known. In our earlier paper[9] the derivative of the dipole tensor was given. The derivative of the modified dipole tensor also includes contributions depending on the derivatives of the screening functions. The modified dipole tensor is given by

$$T_{pq} = \frac{3 f_{pq}^T (\hat{r}_{pq} : \hat{r}_{pq}) - f_{pq}^E}{r_{pq}^3}, \tag{A1}$$

where the distance vector r_{pq} is defined to be the vector from atom q to atom p and r_i is the Cartesian component i of the distance vector. The Cartesian components of the modified dipole tensor can be written as

$$(T_{pq})_{ij} = \frac{3 f_{pq}^T (\hat{r}_{pq;i} \hat{r}_{pq;j}) - f_{pq}^E \delta_{ij}}{r_{pq}^3}. \tag{A2}$$

The derivative of the modified dipole tensor with respect to the coordinate $r_{p;k}$ is then given by

$$\left(\frac{\partial T_{qp}}{\partial r_{p;k}} \right)_{ij} = \frac{3}{r_{pq}^7} (5 r_i r_j r_k - r^2 r_i \delta_{jk} - r^2 r_j \delta_{ki}) f_{pq}^T$$

$$- \frac{3}{r_{pq}^5} r_k \delta_{ij} f_{pq}^E \tag{A3}$$

$$+ \frac{1}{2} \left(\frac{r_i r_j r_k \nu}{r_{pq}^7} - \frac{r_k \delta_{ij}}{r_{pq}^5} \right) \nu^3 \exp(-\nu). \tag{A4}$$

APPENDIX B: SOFT CUTOFF

In our earlier paper, based on the DID model,[9] we noted that noise was generated due to the fact that a molecule in the calculation with applied forces and in the calculation of the background polarizability could be on different sides of the cut-off boundary. Therefore its contribution to the local structure is taken explicitly into account in one calculation but not in the other. This was overcome by making the cut-off distance so large that the contribution from the molecules near the cutoff was vanishing. The problem can be overcome in a more elegant way that also allows using shorter cut-off distances without introducing artifacts due to boundary

J. Chem. Phys., Vol. 116, No. 8, 22 February 2002

Raman response of CS$_2$ 3285

crossing. By introducing a soft cutoff the noise can be reduced. This is done by multiplying the dipole tensor with a weight function that is one at short distances and vanishes beyond the cut-off radius, but is continuous.

We will use a function that is fast to compute and has clear boundaries. Defining the function to be exactly one within the distance $x_c - \Delta x$, where x_c is the cut-off distance and Δx is the cut-off width. Outside the distance $x_c + \Delta x$ the function is defined to be exactly zero, allowing to skip calculations on molecules separated by such distances. In between the function is defined by a polynomial that ensures that both the weight function and its derivative are continuous:

$$
w(x) = \begin{cases} 1 & : x < x_c - \Delta x \\ \dfrac{1}{4}\left(\dfrac{x-x_c}{\Delta x}\right)^3 - \dfrac{3}{4}\dfrac{x-x_c}{\Delta x} + \dfrac{1}{2} & : x_c - \Delta x \leq x \leq x_c + \Delta x \\ 0 & : x > x_c + \Delta x \end{cases}
$$

$$\text{(B1)}$$

The derivative is given by

$$
w^{(1)}(x) = \begin{cases} 0 & : x < x_c - \Delta x \\ \dfrac{3}{4}\left(\left(\dfrac{x-x_c}{\Delta x}\right)^2 - 1\right) & : x_c - \Delta x \leq x \leq x_c + \Delta x \\ 0 & : x > x_c + \Delta x. \end{cases}
$$

$$\text{(B2)}$$

[1] T. Steffen, N. A. C. M. Meinders, and K. Duppen, J. Phys. Chem. A **102**, 4213 (1998).

[2] D. McMorrow, N. Thantu, J. S. Melinger, S. K. Kim, and W. T. Lotshaw, J. Phys. Chem. **100**, 10389 (1996).

[3] S. Ruhman, L. R. Williams, A. G. Joly, and K. A. Nelson, J. Phys. Chem. **91**, 2237 (1987).

[4] A. Waldman, U. Banin, E. Rabani, and S. Ruhman, J. Phys. Chem. **96**, 10840 (1992).

[5] L. C. Geiger and B. M. Ladanyi, J. Chem. Phys. **87**, 191 (1987).

[6] L. C. Geiger and B. M. Ladanyi, Chem. Phys. Lett. **159**, 413 (1989).

[7] R. L. Murry, J. T. Fourkas, and T. Keyes, J. Chem. Phys. **109**, 2814 (1998).

[8] K. Kiyohara, K. Kamada, and Koji Ohta, J. Chem. Phys. **112**(14), 6338 (2000).

[9] T. l. C. Jansen, J. G. Snijders, and K. Duppen, J. Chem. Phys. **114**, 10910 (2001).

[10] X. Ji, H. Alhborn, B. Space, P. B. Moore, Y. Zhou, S. Constantine, and L. D. Ziegler, J. Chem. Phys. **112**, 4186 (2000).

[11] X. Ji, H. Alhborn, B. Space, and P. B. Moore, J. Chem. Phys. **113**(19), 8693 (2000).

[12] T. Keyes and J. T. Fourkas, J. Chem. Phys. **112**, 287 (2000).

[13] A. Tokmakoff, J. Chem. Phys. **105**, 1 (1996).

[14] S. Mukamel, *Principles of Nonlinear Optical Spectroscopy* (Oxford University Press, New York, 1995).

[15] T. Steffen, J. T. Fourkas, and K. Duppen, J. Chem. Phys. **105**, 7364 (1996).

[16] T. Steffen and K. Duppen, J. Chem. Phys. **106**, 3854 (1997).

[17] S. Saito and I. Ohmine, J. Chem. Phys. **108**, 240 (1998).

[18] B. M. Ladanyi, Chem. Phys. Lett. **121**, 351 (1985).

[19] P. A. Madden, in *Ultrafast Phenomena*, Vol. IV, edited by D. H. Auston and K. B. Eisenthal, Vol. IV (Springer, Berlin, 1985), p. 244.

[20] T. l. C. Jansen, J. G. Snijders, and K. Duppen, J. Chem. Phys. **113**(1), 307 (2000).

[21] C. Kalpouzos, D. McMorrow, W. T. Lotshaw, and G. A. Kenney-Wallace, Chem. Phys. Lett. **150**, 138 (1988).

[22] C. Kalpouzos, D. McMorrow, W. T. Lotshaw, and G. A. Kenney-Wallace, Chem. Phys. Lett. **155**, 240 (1989).

[23] J. A. Bucaro and T. A. Litovitz, J. Chem. Phys. **54**, 3846 (1971).

[24] T. Hattori and T. Kobayashi, J. Chem. Phys. **94**(5), 3332 (1991).

[25] A. Idrissi, M. Ricci, P. Bartolini, and R. Righini, J. Chem. Phys. **111**(9), 4148 (1999).

[26] D. McMorrow, N. Thantu, V. Kleiman, J. S. Melinger, and W. T. Lotshaw, J. Chem. Phys. A **105**, 7960 (2001).

[27] N. W. Ashcroft and N. D. Mermin, *Solid State Physics*, (Saunders College, Philadelphia, PA, 1987).

[28] P. T. van Duijnen and M. Swart, J. Phys. Chem. A **102**, 2399 (1998).

[29] M. Swart, P. Th. van Duijnen, and J. G. Snijders, J. Mol. Struct.: THEOCHEM **458**, 11 (1999).

[30] B. T. Thole, Chem. Phys. **59**, 341 (1981).

[31] C. J. F. Böttcher and P. Bordewijk, *Theory of Electric Polarization* (Elsevier, Amsterdam, 1978).

[32] J. A. C. Rullmann and P. Th. van Duijnen, Mol. Phys. **63**, 451 (1988).

[33] E. J. Baerends, D. E. Ellis, and P. Ros, Chem. Phys. **2**, 41 (1973).

[34] G. te Velde and E. J. Baerends, J. Comput. Phys. **99**, 41 (1992).

[35] C. F. Guerra, O. Visser, J. G. Snijders, G. te Velde, and E. J. Baerends, in *Methods and Techniques in Computational Chemistry*, METECC-5, edited by E. Clementi and C. Corongiu (STEF, Cagliari, Italy, 1995).

[36] S. H. Vosko, L. Wilk, and M. Nusair, Can. J. Phys. **58**, 1200 (1980).

[37] S. J. A. van Gisbergen, J. G. Snijders, and E. J. Baerends, Comput. Phys. Commun. **118**, 119 (1999).

[38] G. te Velde, F. M. Bickelhaupt, E. J. Baerends, C. Fonseca Guerra, S. J. A. van Gisbergen, J. G. Snijders, and T. Ziegler, J. Comput. Chem. **22**, 931 (2001).

[39] R. van Leeuwen and E. J. Baerends, Phys. Rev. A **49**, 2421 (1994).

[40] M. P. Bogaard, A. D. Buckingham, R. K. Pierens, and A. H. White, J. Chem. Soc., Faraday Trans. 1 **74**, 3008 (1978).

[41] S. J. A. van Gisbergen, F. Kootstra, P. R. T. Schipper, O. V. Gritsenko, J. G. Snijders, and E. J. Baerends, Phys. Rev. A **57**, 2556 (1998).

[42] V. P. Osinga, S. J. A. van Gisbergen, J. G. Snijders, and E. J. Baerends, J. Chem. Phys. **106**, 5091 (1996).

[43] A. J. Stone, *The Theory of Intermolecular Forces*, International series of monographs on chemistry, Vol. 32 (Oxford University Press, Oxford, 1996).

[44] D. A. Blank, L. J. Kaufman, and G. R. Fleming, J. Chem. Phys. **113**(2), 771 (2000).

[45] M. Khalil, N. Demirdöven, O. Golonzka, C. J. Fecko, and A. Tokmakoff, J. Phys. Chem. A **104**, 5711 (2000).

[46] M. Khalil, O. Golonzka, N. Demirdöven, C. J. Fecko, and A. Tokmakoff, Chem. Phys. Lett. **321**, 231 (2000).

[47] Q.-H. Xu, Y.-Z. Ma, and G. R. Fleming, Chem. Phys. Lett. **338**, 254 (2001).

[48] T. l. C. Jansen, A. Pugzlys, G. D. Grînguş, J. G. Snijders, and K. Duppen, J. Chem. Phys. (unpublished).

[49] D. McMorrow, W. T. Lotshaw, and G. A. Kenney-Wallace, IEEE J. Quantum Electron. **24**(2), 443 (1988).

[50] D. J. Tildesley and P. A. Madden, Mol. Phys. **42**, 1137 (1981).

[51] R. L. Murry, J. T. Fourkas, and T. Keyes, J. Chem. Phys. **109**, 7913 (1998).